RHEOLOGY AND MICROSTRUCTURE OF CONCENTRATED SUSPENSIONS

LISA A. MONDY* AND ALAN L. GRAHAM**
*Sandia National Laboratories, Division 1511, Albuquerque, New Mexico 87185
**Los Alamos National Laboratory, MEE-4, Los Alamos, New Mexico 87545

ABSTRACT

We give an overview of some of the experiments currently underway to study the coupling of the microstructure and rheology of concentrated suspensions. Nuclear magnetic resonance imaging, real-time x-ray radiography, and refractive index matching allow the viewing of particles in concentrated suspensions. Both shear flow experiments and falling ball rheometry are reviewed. In the slow flow of these suspensions of large, hard, particles in a viscous Newtonian fluid, colloidal forces are negligible and hydrodynamic forces dominate.

Large local concentration changes are shown to occur rapidly in suspensions of uniform spheres subjected to flow between concentric rotating cylinders. Suspensions of spheres with a bimodal size distribution not only show similar phenomena, but also exhibit particle separation according to size. In addition, the large particles in the bimodal suspension migrate into ordered, concentric, cylindrical sheets, parallel to the axis of the cylinders. These sheets of particles rotate relative to each other. The particle migration and structure formation induced by this inhomogeneous shear flow is believed to be responsible for torque reductions and other anomalous behavior witnessed during the rheological testing of concentrated suspensions reported in the literature. Thus, suspensions may not always be characterized by a viscosity that is a scalar material property.

Suspensions of fibers also show markedly different rheological properties when the particles are aligned by flow. Falling ball rheometry is shown to be an effective tool to determine the bulk viscosity of a suspension while only slightly influencing the microstructure. This is illustrated by showing that falling ball rheometry can isolate the effect of orientation on the viscosity of a suspension of fibers.

INTRODUCTION

The microstructure of a concentrated suspension influences the macroscopic flow properties of that suspension, and, therefore, affects such processes as injection molding of ceramics or the incorporation of reinforcing fibers into ceramics. In turn, the flow of the suspension influences the microstructure in a tightly coupled process.

Migration and ordering of suspended particles have been hypothesized to cause viscosity measurements that vary with total strain of a sample.[1,2] Microstructural changes in the shear flow of colloidal suspensions of both spheres and fibers have been inferred via light scattering techniques.[3,4] We observe similar phenomena in suspensions of large spheres (600 μm < diameter < 3.2 mm) using nuclear magnetic resonance (NMR) imaging. This noninvasive technique has recently shown great potential in the study of two-phase flow.[5] The experiments discussed in this paper were performed in collaboration with Drs. S. A. Altobelli and Eiichi Fukushima of Lovelace Medical Foundation.

We show that NMR imaging allows the study of flow-induced particle migration in concentrated (solids volume fraction ≥ 0.50) suspensions. Concentration profiles are easily determined, and good spatial resolution obtained. When subjected to flow between

---

rotating concentric cylinders, neutrally buoyant particles migrate away from the inner rotating rod toward the outer fixed cylinder. This migration occurs in suspensions of monodisperse and bidisperse spheres. The monodisperse spheres migrate until the region of lowest shear rate (near the outer wall) contains approximately the maximum concentration of spheres possible for random packing. A similar migration occurs in suspensions of bidisperse spheres. Furthermore, in these bimodal suspensions, concentric bands of larger particles form after shearing. Visual observations of opaque particles in bands near the outer wall of the apparatus show that the larger spheres are arranged in two-dimensional hexagonal close-packed sheets that rotate relative to each other. Ackerson has inferred hexagonal close-packed structure in similar experiments on suspensions of smaller, monodisperse spheres.[4]

This is a dramatic illustration of shear-induced formation of structure in suspensions. If such phenomena are caused by shearing a suspension, then one must confront the need to determine the viscosity of a suspension without *changing* the suspension viscosity through the very act of *measuring* it. Conventional viscometers all employ flow fields that tend to influence the microstructure of the suspension. For example, suspended fibers, if not subject to strong, randomizing, rotary Brownian forces, will tend to align in shearing flow; hence, the measurements will be performed on suspensions having flow-induced anisotropy.

We show that falling ball rheometry may be used to determine the bulk viscosity of a suspension with little effect on the microstructure of the suspension. If the size of the probe (the falling ball) is of the order of the characteristic length of the suspended particles, the ball disturbs the original microstructure of the quiescent suspension only slightly as it falls. We discuss experiments, performed in collaboration with Dr. R. L. Powell of University of California–Davis and Dr. M. Gottlieb of Ben Gurion University, Israel, which illustrate the use of falling ball rheometry to determine the viscosity of suspensions both of randomly oriented rods and of approximately aligned rods. We find that the viscosity in the direction of the aligned rod axes is significantly lower than that with the rods randomly oriented. Furthermore, the viscosity of the oriented rods agrees well with the viscosity measured with rotational rheometers, implying that the rod alignment we set may mimic that induced by shear flow.

NMR imaging experiments showing shear-induced ordering of suspensions of spheres will be detailed in the following section. The third section will discuss real-time radiography and index-matching techniques that allow falling ball rheometry in suspensions of both spheres and fibers. Here, we will discuss falling ball rheometry as a tool to explore the effect of microstructure on the bulk viscosity.

SHEAR-INDUCED DIFFUSION AND CRYSTALLIZATION IN SUSPENSIONS OF SPHERES

NMR Imaging

The distribution of particles and suspending fluid in concentrated suspensions is difficult to measure because observation of the interior of a flow field is obstructed by the high particle density. Most suspensions are opaque even at relatively low particle concentrations. However, the noninvasive method of NMR imaging does allow analysis of the particle distribution profiles in such suspensions. Background material on basic NMR phenomena can be found in standard NMR textbooks.[6,7] Some details of our specific use of NMR imaging techniques will be given in the following paragraphs.

Experiments involving the flow of concentrated suspensions between rotating concentric cylinders currently are being performed in collaboration with Drs. Steve Altobelli and Eichii Fukushima at Lovelace Medical Foundation. They have developed the capability of imaging suspensions using a horizontal bore, superconducting, 1.9 T magnet controlled by a NALORAC, Inc. (Martinez, CA) imaging/spectrometer system. The precisely timed sequence of gradient and rf pulses and data acquisitions used is an adaption of a "spin-warp" technique.[7] A single 100-mm "birdcage" type rf coil[8] generates the rf pulses and detects the NMR signal in these experiments. The signal is extracted from the spectrometer and is processed offline. The original time-domain data are acquired in quadrature and images are calculated from these data by two-dimensional Fourier transformation. Each time-domain data set is a 128 by 128 complex array obtained by averaging the results of four to eight phase-cycled image acquisition sequences to optimize the signal-to-noise ratio. The modulus of each resulting picture element of the image is mapped to intensity or color for display.

The fluid in the imaged slice of sample gives a full-intensity signal and the particles give no signal. The normalized value of the image intensity is proportional to the density of the liquid phase protons in a volume element. The NMR image then can not only provide visualization of the particle structure but also quantitative information about the concentration of particles as a function of location.

The Couette Flow Experiments

We will discuss the results obtained when two highly concentrated, model suspensions were subjected to wide-gap, annular, Couette flow. Both suspensions consisted of polymethyl methacrylate (PMMA) spheres in a Newtonian oil. The spheres in the first suspension were approximately monodisperse with a mean diameter of 600 μm. The spheres in the second suspension were a mixture of 720-μm-mean-diameter spheres and individually ground, 3.175-mm-diameter spheres (Clifton Plastics Company) to form a bimodal size distribution. Thirty-five percent of the particles in this suspension were the small spheres and 65% were the large spheres. Total solids contents of the two suspensions were 50 vol% and 60 vol% for the suspensions with monomodal and bimodal size distributions, respectively.

The Newtonian suspending liquid used is discussed in detail in the section entitled "Refractive Index Matching to Produce Transparent Suspensions". This composition was chosen to match the density of the PMMA spheres at 21.5°C (1.185 g/cm^3). Although the temperature of each suspension was controlled only by the room air conditioner, no settling of the suspended particles was detected over the duration of the experiments. This liquid has been used in our laboratory in experiments based on optical techniques because it also matches the refractive index of the PMMA; however, this property is not necessary when using the NMR technique. The viscosity of the suspending liquid was 4.95 Pa·s at 21.5°C.

Two concentric cylinder (Couette) devices were built. Each consisted of a rotating solid PMMA cylinder concentric in a fixed outer PMMA tube capped with solid PMMA disks. These were wide-gap Couette devices designed to produce an inhomogeneous shear field in the gap. The gap sizes used corresponded to about 32 times the diameter of the particles in the monomodal suspension and about 7 times the diameter of the large spheres in the bimodal suspension. The inner rod was turned at approximately 48 rpm by a variable speed motor. This gave shear rates from about 1 to 10 sec^{-1} (assuming a Newtonian fluid response) across the gap of either apparatus.

The motor was stopped periodically and NMR images were taken of the resulting particle structure. Because buouyancy, Brownian, and surface forces were negligible in these suspensions, no particle movement was expected to occur in the few minutes it took to collect an NMR image. End effects were minimized by making the length-to-diameter ratio of the device sufficiently large and examining each sample specimen near its center. Images were taken of a cross section of the Couette, perpendicular to the Couette axis, about midway along the apparatus. This slice was 24 mm thick in the axial direction.

For each image the centroid of the image was computed, corresponding to the Couette axis. Then the average values of the image intensity in concentric annuli about the centroid were computed. These values were normalized so that the average intensity of the image depicting the initial state matched the known fluid fraction. Thus, with this relative calibration we could estimate the fluid fraction in each concentric annuli of each image, giving the fluid fraction as a function of radius and time (or strain).

The resulting information on fluid fraction as a function of radial distance from the axis of the device showed that substantial particle migration away from the inner rod began to happen immediately upon rotation of the inner rod. With the monomodal suspension, the inner rod was stopped for the first time after 10 revolutions and NMR images were taken. The fluid fraction near the inner rod increased noticeably after only 10 revolutions of the inner rod. The radial distribution of particles did not appear to change substantially after 2500 revolutions. The data taken at this point, apparently at steady state, indicate that the fluid fraction had reached a low of about 0.40 at the outer cylinder. This corresponds to a solids fraction of about 0.60, a value near the maximum value for random packing of monodisperse spheres. However, details of the packing structure for monodisperse spheres will have to wait for the results of experiments currently underway using higher resolution NMR imaging on suspensions of larger monodisperse particles.

After steady state was obtained with clockwise revolutions of the inner rod, the motor was reversed and the inner rod was rotated counterclockwise for approximately the same number of revolutions. The data remained unchanged with the reverse rotation, and, therefore, the particle-concentration distribution remained at the steady-state value. This irreversibility is consistent with the proposed mechanisms of shear-induced migration of particles or "hydrodynamic diffusion" down a shear-field gradient.[1,9]

The particle migration occurred almost entirely in the radial direction. No significant axial migration of colored marker particles was detected in the bimodal suspension. Furthermore, NMR images taken near the ends of the Couette device were not noticeably different from those taken at the center of the device.

For the suspension of spheres with a bimodal size distribution, changes in the concentration profile of the suspension were again seen very quickly upon rotating the inner rod. The initial and final images are shown in Figure 1, with the light areas indicating the presence of liquid. Individual large spheres can almost be distinguished, although the thickness of the imaged volume results in a blurring of the particles. The initial state looks relatively uniform with the particles dispersed randomly. In the final image, the bright area near the inner cylinder represents a higher fluid fraction, indicating that the fluid fraction is significantly higher near the inner rod (the region of highest shear rate) and lower near the outer cylinder. In addition, definite indications of structure can be seen as the fluid fraction oscillates rather than decreases monotonically with radial position. We can see distinct bands of larger spheres interspersed with fluid and smaller spheres. From visual observations of the band near the outer wall of the apparatus, the larger spheres in this layer appear to be hexagonal close-packed. Although individual small spheres cannot be distinguished at this resolution, we infer from the concentration data that the smaller particles are interspersed throughout the suspension but are predominantly in the regions

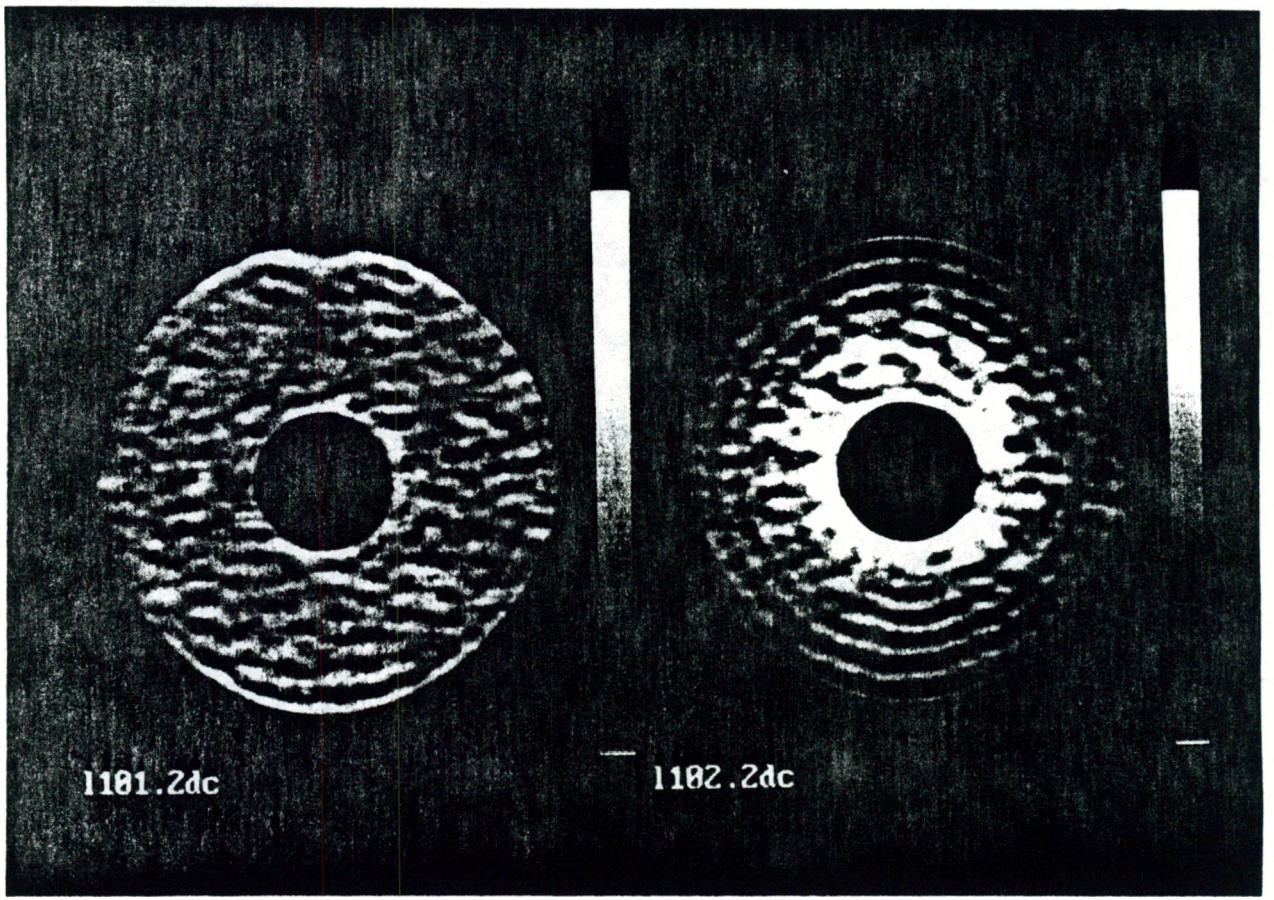

Figure 1. NMR images of a cross section of the suspension of 60 vol% bidisperse spheres between concentric cylinders. The image on the left represents the initially well dispersed state of the suspension. The image on the right was taken after rotating the inner cylinder until steady state was achieved.

between the outermost layers of large spheres. One way to look at this phenomenon is to consider the concentric shells to be formed in order to minimize the force necessary to turn the center rod. This conjecture is corroborated by our observation that the torque required to turn the center rod decreases with increasing number of rotations until steady state is achieved.

FALLING BALL RHEOMETRY IN CONCENTRATED SUSPENSIONS

Real-Time X-Ray Radiography

Radiography using penetrating radiation such as x rays is another method to image opaque suspensions. If the imaging is on a fluor, the image may be electronically amplified, observed by a video camera, and recorded on videotape. This technique allows the tracking of high-Z-number tracer particles within the suspension.

We have used a variety of x-ray generators in this technique. Most commonly we use a fixed x-ray generator, manufactured by Philips, to produce a beam with a 150 kV constant potential, a 20 mA current, and a 1.2 mm focal spot size. The beam is collimated to limit the radiation beam to the area of inspection, minimizing unwanted, scattered radiation that could interact with the fluor and degrade the image. A high-energy x-ray image intensifier, manufactured by Science Application Inc., is used to convert the x-rays to light. This system offers a choice of three sizes (100, 150, or 230 mm diameter) for the x-ray field of view. Once formed, the radiographic image is viewed by a video camera placed at the output of the image intensifier. Video recording of the image allows immediate playback of the event.

The use of two complete x-ray systems focused on the same point provides a stereo view of the tracer particles for three-dimensional tracking. The video system can support two cameras simultaneously. The use of split-screen recording ensures the synchronization of the two images. With this stereo view, we obtain four screen coordinates to determine three spatial coordinates of the centroid. This is an overdetermined systems problem that lends itself to linear regression analysis. In collaboration with Prof. Howard Brenner and Mr. James R. Abbott, both of M.I.T., we have used the process described by Walton[10] to determine the laboratory-fixed coordinates from the camera coordinates.

The accuracy in laboratory space depends on the field of view, determined by the needs of the particular experiment. In the experiments on model suspensions, discussed in the following subsections, an area about 150 × 75 mm is imaged on each split screen. This implies that the accuracy in the measured position of the particle is within 0.02 cm. (However, note that with an x-ray microfocus, a typical field of view is only 10 mm × 10 mm, and very small particles can be tracked accurately. We have successfully tracked steel balls with diameters of 432 μm, both while they were settling in a propellant simulant and while they were moving with the simulant in capillary flow.[11])

Refractive Index Matching to Produce Transparent Suspensions

Although real-time radiography has the distinct advantage that it can be used with any opaque suspension, the tracking of tracer particles can be accomplished optically in a transparent suspension. We have developed the three-component, Newtonian liquid, mentioned previously, that matches both the refractive index and the density of PMMA. Therefore, transparent suspensions of neutrally buoyant PMMA particles can be made.

This suspending liquid is a solution of practical grade 1,1,2,2 tetrabromoethane (TBE) from Eastman Kodak (14.07% by weight); UCON oil (H-90,000), a polyalkylene glycol made by Union Carbide (35.66% by weight); and Triton X-100, an alkylaryl polyether alcohol from J. T. Baker (50.27% by weight). A small amount (about 0.1% of the weight of TBE) of Tinuvin 328, made by Ciba-Giegy, is dissolved in the TBE before mixing to prevent the breakdown of TBE when it is subjected to UV radiation. Similar solutions with various viscosities can be made by using different UCON oils, which can be purchased in a wide range of viscosities.

Falling Ball Experiments and Suspensions of Spheres

Both of the methods discussed above have been used by us and by our coworkers to track the path of a dense sphere settling slowly through a quiescent suspension. In a single-phase Newtonian liquid, the terminal velocity of the sphere is directly related to the liquid viscosity by Stokes' law,[12] corrected, if needed, for the increased drag on the sphere that occurs because of the presence of the container walls.[13] In a suspension an apparent viscosity can be measured as if the suspension were representable as a hypothetical Newtonian liquid.[14]

We have measured the viscosities of suspensions of 5% to 55% by volume of uniform PMMA spheres in various density-matched Newtonian liquids, usually a mixture of UCON oil and TBE. Suspended spheres from 3.18 mm to 12.7 mm in diameter have been used. A ball composed of any metal such as brass, nickel, or tungsten carbide is a sufficient x-ray attenuator, relative to the liquid, the suspended particles, and the container, to produce an x-ray image that can be tracked as the ball falls through the suspension. Balls of opaque plastic, glass, aluminum, and corrundum have also been used in transparent suspensions. Typically, we use balls of a size fairly close to that of the suspended spheres. The suspensions are held in temperature-controlled cylindrical columns and are stirred before each experiment to achieve a uniform distribution of suspended particles.

The discrete nature of the suspension is readily apparent in falling ball experiments. We observe that a large ball falls smoothly through a suspension of smaller particles and its velocity appears fairly constant. Passage of a ball of the same diameter as the suspended particles is extremely erratic. Periods of almost no motion, as the falling ball approaches and "rolls off" suspended particles, alternate with periods of almost free fall in the interstices between suspended spheres. However, a statistical analysis reveals that the *average* terminal velocity of the ball, measured over a distance (usually between 100 and 1000 suspended particle diameters), is reproducible.

Furthermore, if this terminal velocity, corrected for Newtonian wall effects, is translated into a viscosity, this viscosity is independent of the size of the falling ball relative to the diameter of the suspended spheres over a wide range of falling ball sizes. (Anomalous behavior can occur with very small or very large balls, though.[15,16]) For moderately concentrated suspensions (below about 30% solids), the average relative viscosity (η_r, the viscosity of the suspension normalized by the suspending fluid viscosity), agrees with independent measurements taken in shear and capillary rheometers[17] (Figure 2). These rheometers generally indicate that moderately concentrated suspensions of spheres behave as Newtonian fluids, without the anomalous strain-dependent results of the higher concentrations. Therefore, the falling balls experience the same average resistance to motion that they would experience if the effects of the numerous surrounding spheres were replaced by a hypothetical, Newtonian, one-phase fluid, characterized by the suspension viscosity.

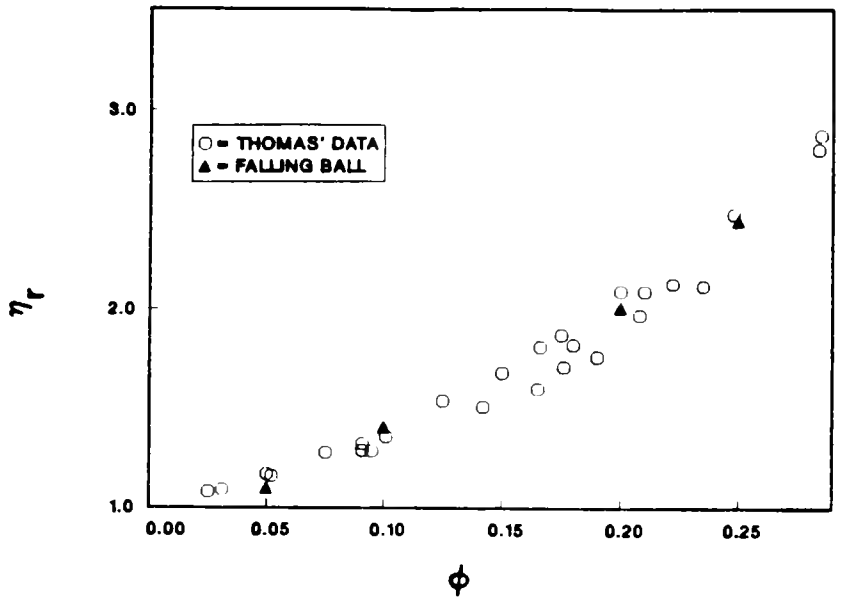

Figure 2. Comparison among the relative viscosities of spherical particle suspensions measured using falling ball rheometry and those measured using shear and capillary rheometers.[17]

Falling ball rheometry, using relatively small balls, then can determine the bulk shear viscosity of a suspension *while only slightly modifying the suspended particle distribution.* In collaboration with Professor Brenner and Mr. Abbott, we are exploring the possibility of using the fluctuations in the terminal velocity, as the ball interacts with individual suspended particles or clusters of suspended particles, to give information about the suspension microstructure.

Falling Ball Experiments and Suspensions of Rods

An illustration of the use of falling ball rheometry as a tool to measure viscosity without unduly influencing the microstructure of the suspension can be found in recent work with suspensions of rodlike particles.[18–20] For suspensions of non-Brownian rods in Newtonian fluids, viscometric and elongational flows, the usual tools of rheologists, induce an alignment of the rods. With falling ball rheometry the initial orientational distribution of the rods can be controlled and fiber-aligning effects of the flow field are minimal.

Experiments were performed in collaboration with Drs. W. J. Milliken, R. L. Powell, and M. Gottlieb to determine the macroscopic viscosity of suspensions of randomly oriented rods.[18,19] Large rods (typically 1.596-mm diameter) were suspended in density-matched Newtonian liquids. The particles were well characterized, and suspensions with various particle aspect ratios and concentrations were tested. As in the tests with suspension of spheres, the suspensions were placed in temperature-controlled cylindrical columns and were stirred before each experiment to achieve a random distribution of particles. The average viscosity given by a ball of specific size was determined by measuring the terminal velocity of at least 10 or 20 identical balls. Again, balls of various sizes all yielded the same average viscosity.

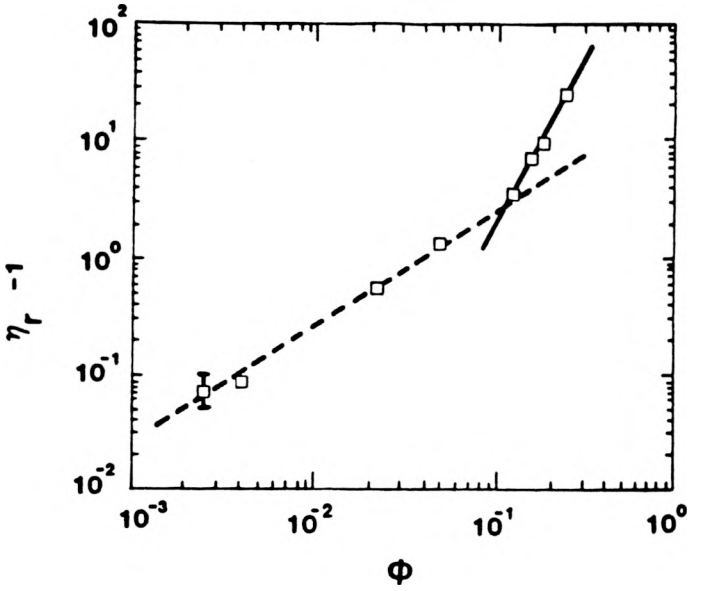

Figure 3. Specific viscosity (measured with falling ball rheometry) of suspensions with various volume fractions (ϕ) of randomly oriented, aspect-ratio-19.83 rods. The equations representing the least-squares fits (the dashed and solid lines) to the data are $\eta_r - 1 = 28.5\phi^{1.01}$ for $\phi < 0.125$ and $\eta_r - 1 = 2040\phi^{3.01}$ for $\phi > 0.125$.

The principal results of experiments using suspended rods with aspect ratio of 19.83 are shown in terms of the specific viscosity ($\eta_r - 1$) in Figure 3. The viscosities of the suspensions vary linearly with solids volume fraction below a volume fraction of about 0.125. Therefore, linear behavior is observed at volume fractions much higher than previously expected and considerably higher than is found with suspensions of spherical particles. However, this critical volume fraction where the transition between dilute (linear) and (semi)concentrated behavior occurs is remarkably similar to that predicted for solutions of rodlike macromolecules, as is the dependence of the specific viscosity on the cube of the concentration after this transition.[21–23] Steric effects, present both in the solutions of macromolecules and the suspensions, may account for the similarity in behavior.

Unlike with suspensions of spherical particles, here we cannot compare the falling ball measurements with shear flow measurements because the latter measurements cannot be done on a similar suspension of *randomly distributed* rods. The flow necessarily sets up a different structure of particles in the suspension. However, theoretical predictions by Brenner exist for suspensions of rods subject to strong Brownian motion.[24] Furthermore, the work by Haber and Brenner shows that these suspensions of Brownian rods behave in shear flow exactly as would suspensions with sustained random distributions of particles.[25] Therefore, we can compare these experiments at large Peclet numbers with the theory for Brownian particles. The intrinsic viscosity predicted by Brenner for suspensions of rods of this aspect ratio is 29.2, and the experimental results of 27.6 differ from this by only 5.8%. Further experiments with other aspect ratio rods also show very good agreement with theory.[19,26]

In these falling ball measurements, the suspensions were stirred before each experiment to ensure that the suspensions were isotropic. In a following series of experiments, the suspended rods were approximately aligned before each measurement so that the suspensions were anisotropic.[20] The large, neutrally buoyant rods were oriented hydrodynamically by passing a fixture through the suspension. This produced a local flow that tended to align the particles along the axis of the column containing the suspension. Here,

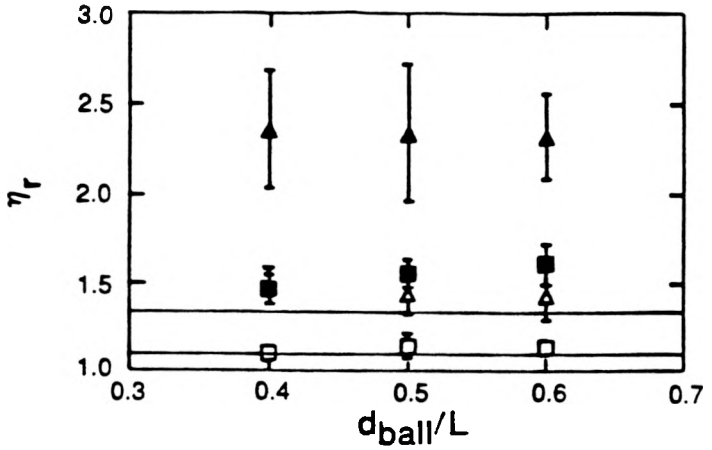

Figure 4. The relative viscosity vs. dimensionless ball diameter (diameter of the falling ball divided by the length of the suspended rods) for suspensions of aligned rods as measured using falling ball rheometry. Suspensions of various volume fractions are represented: $\phi = 0.02$ (□), $\phi = 0.05$ (△). Also shown are the relative viscosities of suspensions of randomly oriented rods: $\phi = 0.02$ (■), $\phi = 0.05$ (▲), and lines representing data obtained in shearing flows.

the falling ball measurements yielded an apparent viscosity (in the direction parallel to the axis of the cylinder) that was substantially less than that for a suspension having the same volume fraction of the same rods in a random configuration. The results are shown in Figure 4. In addition, the viscosities measured for the suspension of aligned rods closely correlated with the viscosities of suspensions of short fibers (having similar aspect ratios and concentrations) measured in shearing flows.[27] This implied that such alignment may mimic the flow-induced orientation found in rotational rheometers. These results showed the possibility of using falling ball rheometry to determine a viscosity dependent on the measurement direction (a viscosity *tensor*) for anisotropic suspensions.

CONCLUSIONS

With techniques such as NMR imaging, real-time radiography and refractive-index matching, we have been able to view the movement of particles in concentrated suspensions. Experiments using these techniques have shown that suspensions may not always be characterized by a scalar material property such as the term "viscosity" implies. Instead, flow may induce particle arrangements that affect the bulk flow properties of the suspension. In other words, the suspension would yield different measured macroscopic viscosities in different flow fields. We have presented here an illustration of flow-induced structure in the form of NMR images taken of a concentrated suspension undergoing inhomogeneous shear in a wide-gap Couette apparatus. The measurements of viscosity taken in such a flow field would depend on the total strain and, hence, on the time of the measurement, until a steady-state particle arrangement formed.

In contrast, falling ball measurements show that a *homogeneous isotropic* suspension often behaves as would a single-phase Newtonian liquid. These measurements, however, have little effect on the structure of the suspension because the probe (the falling ball) size is fairly small compared with the size of the suspended particles. Experiments using suspensions of rods illustrate that falling ball rheometry may be a useful tool to isolate the effects of particle orientation on the bulk viscosity and, furthermore, to probe the relationship between the suspension microstructure and its macroscopic properties.

ACKNOWLEDGMENTS

Many colleagues not explicitly mentioned in the text were also involved in various aspects of the work presented here. In chronological order they were Ms. Julie Jensen, Mr. Larry Bryant, Jr., Ms. Laura Price, Mr. T. G. Morrison, Dr. Thomas S. Stephens, Lt. Wayne J. Tetlow, Lt. James E. Breck, and Mr. Raffy Mor.

This work was sponsored by the U. S. Department of Energy, at Los Alamos National Laboratory under Contract W-7405-ENG-36 with the University of California and at Sandia National Laboratories under Contract DE-AC04-76DP00789. The authors would like gratefully to acknowledge partial support for this work by the U.S. Department of Energy, Division of Engineering and Geosciences, Office of Basic Energy Sciences. Work at Los Alamos National Laboratory was also partially supported by the Air Force Astronautics Laboratory, Edwards AFB, CA.

REFERENCES

1. D. Leighton and A. Acrivos, *J. Fluid Mech.*, **181**, 415 (1987).

2. R. D. Surovec, D. M. Husband, T. S. Stephens, and A. L. Graham, "Reproducibility in Measuring Rheology of Highly Concentrated Suspensions," JANNAF Propellant Development Characterization Subcommittee 1989 Annual Meeting, Laurel, Maryland, 1989.

3. A. J. Salem and G. G. Fuller, *J. Colloid Interface Sci.*, **108**, 149 (1985).

4. B. J. Ackerson and P. N. Pusey, *Phys. Rev. Lett.*, **61**, 1033 (1988).

5. P. D. Majors, R. C. Givler, and E. Fukushima, *J. Magnetic Resonance*, **85**, 235 (1989).

6. P. G. Morris, *Nuclear Magnetic Resonance Imaging in Medicine and Biology*, Clarendon Press, Oxford, 1986.

7. A. Abragam, *The Principles of Nuclear Magnetism*, Clarendon Press, Oxford, 1961.

8. J. C. Watkins and E. Fukushima, *Rev. Sci. Instrum.*, **59**, 926 (1988).

9. D. L. Koch, *Phys. Fluids A*, **1**, 1742 (1989).

10. J. S. Walton, "Close-Range Cine-Photogrammetry," Thesis, Penn State University (1981).

11. A. L. Graham, L. A. Mondy, and R. L. Powell, "Applications of Real-Time Radiography to Rheological Characterization and Processing Dynamics," JANNAF Propellant Development Characterization Subcommittee 1987 Annual Meeting, Laurel, Maryland, 1987.

12. R. B. Bird, W. E. Stewart, and E. N. Lightfoot, *Transport Phenomena* (John Wiley & Sons, New York, 1960), p. 59.

13. T. Bohlin, *Trans. R. Inst. Tech. (Stockholm)*, No. 155.

14. L. A. Mondy, A. L. Graham, and J. L. Jensen, *J. Rheol.*, **30**, 1031 (1986).

15. W. J. Milliken, L. A. Mondy, M. Gottlieb, A. L. Graham, and R. L. Powell, *PCH PhysicoChemical Hydrodynamics*, **11**, 341 (1989).

16. L. A. Mondy, A. L. Graham, and M. Gottlieb, "Microrheological Observations on the Onset of Non-Newtonian Behavior in Suspensions," Xth International Congress on Rheology, Sydney, Australia, August 1988.

17. D. G. Thomas, *J. Colloid Sci.*, **20**, 267 (1965).

18. W. J. Milliken, M. Gottlieb, A. L. Graham, L. A. Mondy, and R. L. Powell, *J. Fluid Mech.*, **202**, 217 (1989).

19. R. L. Powell, L. A. Mondy, G. G. Stoker, W. J. Milliken, and A. L. Graham, *J. Rheol.*, **33**, 1173 (1989).

20. L. A. Mondy, T. G. Morrison, A. L. Graham, and R. L. Powell, *Int. J. Multiphase Flow*, (in press 1990).

21. M. Doi and S. F. Edwards, *J. Chem. Soc. Faraday Trans. II*, **74**, 918 (1978).

22. G. T. Keep and R. Pecora, *Macromol.*,**18**, 1167 (1985).

23. J. J. Magda, H. T. Davis, and M. Tirrell, *J. Chem. Phys.*, **85**, 6674 (1986).

24. H. Brenner, *Intl. J. Multiphase Flow*, **1**, 195 (1974).

25. S. Haber and H. Brenner, *J. Colloid Interface Sci.*, **97**, 496 (1984).

26. Morrison, T. G., M.S. thesis, University of California – Davis, 1989.

27. E. Ganani and R. L. Powell, *J. Rheol*, **30**, 995 (1986).

DISCLAIMER